Solution Properties of Chitin in Alkali

ARTICLE *in* BIOMACROMOLECULES · SEPTEMBER 2004

Impact Factor: 5.75 · DOI: 10.1021/bm049710d · Source: PubMed

Solution Properties of Chitin in Alkali

Aslak Einbu,[†] Stine Nalum Naess,[‡] Arnljot Elgsaeter,[‡] and Kjell M. Vårum*,[†]

Department of Biotechnology and Department of Physics, Norwegian University of Science and Technology (NTNU), N-7491 Trondheim, Norway

Received May 14, 2004; Revised Manuscript Received July 9, 2004

The solution properties of α-chitin dissolved in 2.77 M NaOH are discussed. Chitin samples in the weight-average molecular weight range 0.1×10^6 g/mol to 1.2×10^6 g/mol were prepared by heterogeneous acid hydrolysis of chitin. Dilute solution properties were measured by viscometry and light scattering. From dynamic light scattering data, relative similar size distributions of the chitin samples were obtained, except for the most degraded sample, which contained aggregates. Second virial coefficients in the range 1 to 2×10^{-3} mL·mol·g^{-2} indicated that 2.77 M NaOH is a good solvent to chitin. The Mark−Houwink−Sakurada equation and the relationship between the *z*-average radius of gyration (R_g) and the weight-average molecular weight (M_w) were determined to be $[\eta] = 0.10M_w^{0.68}$ (mL·g^{-1}) and $R_g = 0.17M_w^{0.46}$ (nm), respectively, suggesting a random-coil structure for the chitin molecules in alkali conditions. These random-coil structures have Kuhn lengths in the range 23−26 nm.

1. Introduction

Chitin is one of the most abundant of all biopolymers and is found mainly as a structural polysaccharide in arthropod cuticles where it constitutes one of the three major components together with proteins and $CaCO_3$. It is a linear polysaccharide composed of β-(1−4)-linked 2-acetamido-2-deoxy-D-glucose units which may be de-*N*-acetylated to some extent. Chitin is like cellulose: insoluble in dilute aqueous solvents and common organic solvents. However, both chitin and cellulose are soluble in *N*,*N*-dimethylacetamide (DMAc)−LiCl.[1] Chitin can be dissolved when an alkaline suspension of the polymer is mixed with ice.[2] Using chitin samples of various molecular weights, we have undertaken a study of the solution properties of chitin in 2.77 M NaOH.

The intrinsic viscosity $[\eta]$ of a polymer in solution is related to the molecular weight *M* by the Mark−Houwink−Sakurada (MHS) equation

$$[\eta] = KM^a \tag{1}$$

The values of the parameters *K* and *a* depend on both the polymer−solvent system and the temperature.[3] The exponent *a* is a polymer conformation parameter that decreases with increasing molecular compactness. For extended rodlike molecules, the value is larger than 1. For random-coil molecules, $a = 0.5$ in a poor solvent and 0.8 in a good solvent. For compact, spherical molecules $a = 0$. The solution properties of cellulose in DMAc−LiCl have been studied,[4] and it was found that $a = 1.19$. The exponent *b* in the relation between the *z*-average radius of gyration R_g and the weight-average molecular weight M_w, $R_g = CM_w^b$, was determined to 0.74. The radius of gyration and the molecular weight were used to calculate the characteristic ratio and the persistence length. The authors concluded that the DMAc−LiCl solvent greatly enhances the stiffness of the cellulose backbone.[4] From light scattering and viscosity studies of chitin dissolved in DMAc−LiCl, the following relationships were obtained:[5] $R_g = 0.024M_w^{0.64}$ nm and $[\eta] = 0.0024M_w^{0.69}$ (dL/g). Using the Yamakawa−Fujii and Benoit−Doty expressions for wormlike chains, values of the persistence length from 15 to 50 nm were calculated, depending on the method of calculation.

For a polydisperse system, the MHS equation yields the viscosity-average molecular weight, M_v. The viscosity-average molecular weight is generally closer to the weight-average molecular weight, M_w, than the number-average molecular weight, M_n. Therefore, absolute methods yielding M_w (light scattering and sedimentation measurements) should be preferred to those yielding M_n (osmotic pressure measurements and end group determination) in the calibration of the $[\eta]-M$ dependency. Once *K* and *a* have been established for a given polymer−solvent system at a specific temperature, the correct M_w of an unknown sample with known $[\eta]$ can be determined. If the polymer in question is polydisperse with respect to the molecular weight, the unknown sample must have the same molecular weight distribution as the samples used to calibrate the MHS equation.

2. Experimental Section

2.1. Preparing Samples of Alkali Chitin. Chitin was isolated from shrimp shells by removing $CaCO_3$ with cold 0.25 M HCl for 30 min prior to treatment with 1 M NaOH at 95 °C for 5 h to remove the protein fraction of the shell. The fraction of acetylated units F_A of chitin was determined with ^{1}H NMR on chitin dissolved in concentrated DCl by

* Corresponding author. E-mail: kjell.morten.vaarum@biotech.ntnu.no. Tel.: +47-73593324. Fax: +47-73591283.

[†] Department of Biotechnology, Norwegian University of Science and Technology.

[‡] Department of Physics, Norwegian University of Science and Technology.

10.1021/bm049710d CCC: $27.50
Published on Web 08/19/2004

the method described by Einbu and Vårum.[6] The value of the parameter F_A of the isolated chitin was determined to equal 0.96.

Powdered chitin was suspended in 40% (w/w) NaOH and kept at 4 °C for 72 h. The suspension was then mixed with finely crushed ice (precooled in a freezer before use) and stirred while being cooled in an ice bath. The result was a rather viscous solution of 2.25 mg/mL chitin in 10% (w/w) NaOH. To investigate possible degradation of the sample caused by shear forces during the dissolution, different amounts of stirring and shaking were applied to different dissolutions of a high-molecular-weight chitin sample. Light scattering measurements of these samples showed no significant difference in molecular weight. Consequently, the shear forces during the dissolution process do not cause degradation of the sample.

The samples were filtered using 0.45 μm filters (Versapor Membrane, PALL Gelman Laboratory) and kept on ice before being examined by light scattering and viscometric measurements. All measurements were performed within a maximum of 6 h after the samples had been prepared. Both the viscometric and light scattering measurements were carried out at 20 °C. To determine F_A in a sample of alkali chitin, the alkali chitin was precipitated by adding 3 M HCl to pH 7 before washing with distilled water prior to analysis.

Chitin samples were heterogeneously hydrolyzed to different molecular weights by treatment in 3 M HCl at 25 °C for 3, 12, 24, 48, and 345 h, respectively. The value of parameter F_A for the untreated sample was determined to be 0.96 while F_A of the sample treated with acid for 345 h was 0.91. The chitin samples are denoted C-1 (lowest M_w) to C-6 (highest M_w).

2.2. Light Scattering. The light scattering measurements were performed using an ALV DLS/SLS-5022F compact goniometer system and ALV-5000/E multiple τ digital correlator (ALV, Langen, Germany). The alignment of the instrument was repeatedly checked by measuring the static light scattering of toluene. For scattering angles ranging from 20 to 154°, the scattered intensity showed less than 1% deviation from the expected 1/sin θ dependence.[7] The light source was a 22-mW vertical polarized He−Ne laser (Uniphase, Witney Oxon, U.K.) of wavelength 632.8 nm. The scattering angles used in the static light scattering measurements range from 30 to 150°. For measurements of dynamic light scattering, a scattering angle of 90° was used. The concentration of chitin varied from 0.05 to 2.25 mg/mL. The samples were carefully filtered with 0.45-μm filters (Versapor Membrane, PALL Gelman Laboratory) directly into the light scattering cuvettes, unless otherwise specified. The specific refractive index increment $\partial n/\partial c$ of alkali chitin was 0.145 mL/g based on measurements carried out on chitosan solutions at pH 4.5.[8]

The uncertainty in the light scattering measurements was determined by performing measurements on different stock solutions made from chitin sample C-6. Sample C-6 represents the sample of highest molecular weight and, therefore, the sample most difficult to dissolve in alkali. In this way, the uncertainty originating from the preparation of the chitin sample was incorporated into the estimated uncertainties.

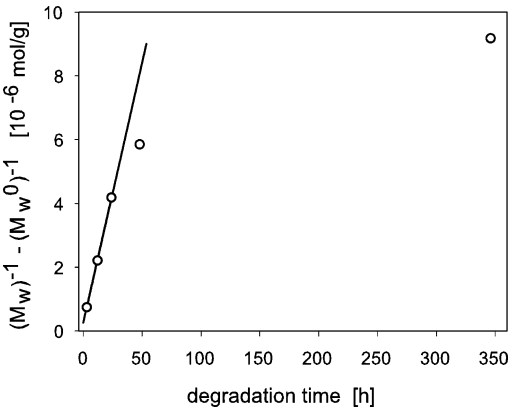

Figure 1. Plot of $(1/M_w - 1/M_w^0)$ versus degradation time at 25 °C for the chitin samples in 3 M HCl. The molecular weights were determined by static light scattering measurements of alkali chitin.

From Zimm plots, the uncertainty in the molecular weight, radius of gyration, and second virial coefficient were determined to be 6.5, 5.4, and 12.5%, respectively.

2.3. Viscometry. The viscosity measurements were performed using a Schott-Gerate Ubbelohde viscometer (Type 536 10/I). All calculations were based on chitin solutions of relative viscosity $\eta_{rel} \leq 2$. To obtain more accurate values, the intrinsic viscosities were determined as the average of extrapolating both η_{sp}/c and log η_{rel}/c to 0 concentration.[9]

The uncertainty in the intrinsic viscosity was determined by performing measurements on different stock solutions made from chitin sample C-2. Sample C-2 is the second lowest in molecular weight of the studied samples and has some of the fastest flow times in the viscometer. The uncertainty in the intrinsic viscosity was determined to be 4.2%.

3. Results and Discussion

3.1. Heterogeneous Hydrolysis of Chitin. The random depolymerization of a single-stranded polymer can be described by the relation

$$\frac{1}{M_w} = \frac{1}{M_w^0} + kt \qquad (2)$$

where t denotes the reaction time, k is the rate constant, and M_w^0 is the molecular weight at $t = 0$. A plot of $(1/M_w) - (1/M_w^0)$ versus degradation time is given in Figure 1. Initially, the values of $(1/M_w) - (1/M_w^0)$ increase proportionally with time, indicating a random depolymerization reaction. This will result in a Kuhn distribution of the molecular weight. However, for reaction times longer than 24 h, the values deviate significantly from the initial straight line. The deviation cannot be explained by a loss of a low-molecular-weight fraction during the sample preparation, because the yield, that is, the ratio of chitin before and after acid hydrolysis, was the same for all samples of different molecular weights.

A possible explanation for these results could be that the chitin structure consists of both amorphous and crystalline regions.[10] The amorphous regions are more accessible for acid hydrolysis than the crystalline regions, and a selective fast degradation of the amorphous regions will result in a

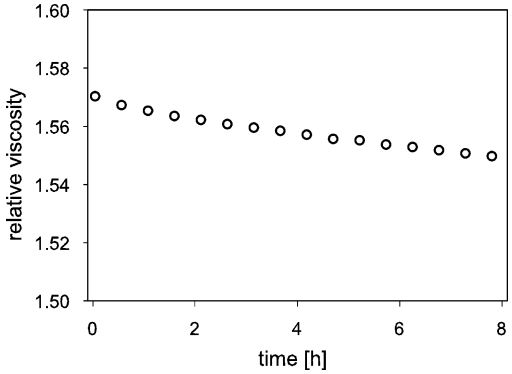

Figure 2. Relative viscosity, η_{rel}, of chitin sample C-5 in alkali as a function of time (c = 0.5 mg/mL, 20 °C).

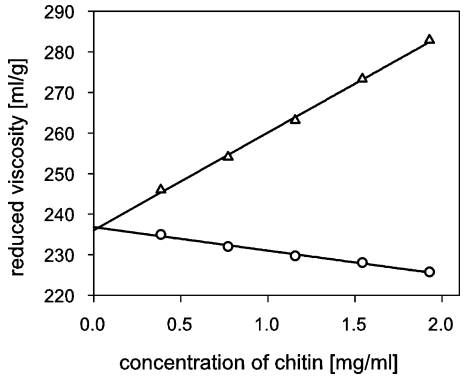

Figure 3. Determination of intrinsic viscosity of chitin sample C-1 in alkali by plotting η_{sp}/c (△) and $\log\eta_{rel}/c$ (○) versus concentration and extrapolation to zero concentration ($[\eta]$ = 237 mL/g, 20 °C).

high-molecular-weight fraction of slow degradable crystalline chitin. This high-molecular-weight fraction will significantly contribute to the measured weight-average molecular weight in static light scattering. Even though the degradation is much slower in crystalline regions than in amorphous regions, it will initially appear as random, because of the relatively small number of broken glycosidic bonds, as shown in Figure 1.

3.2. Chemical Stability of Chitin Dissolved in Alkali. To investigate possible degradation of chitin in alkali, the relative viscosity was measured for 8 h at 20 °C (Figure 2). Over this time period, the relative viscosity decreased from 1.57 to 1.55, which indicated no significant change in the molecular weight.

To investigate possible deacetylation of chitin in alkali, F_A was determined in chitin sample C-1, which was precipitated after 8 h. We found that F_A decreased from 0.91 to 0.85. The result shows that chitin in alkali is stable with respect to degradation. A limited decrease in F_A as a result of both acid and alkaline hydrolyses can be detected during the time span of our experiments.

3.3. Determination of Intrinsic Viscosity. For each chitin sample, the relative viscosities of several solutions with different concentrations were measured in a capillary viscosimeter. Values of the specific viscosity divided by the chitin concentration, η_{sp}/c, and $\log \eta_{rel}/c$ were plotted versus concentration. The intrinsic viscosity was calculated by an average of η_{sp}/c and $\log \eta_{rel}/c$ extrapolated to infinite dilution, as shown in Figure 3.

To determine whether the samples showed Newtonian behavior or not, viscosity measurements were performed on the chitin sample C-6 in alkali using a StressTech rheometer (Reologica, Lund, Sweden). Measurements were carried out on a double gap geometry plate at 20 °C with shear rates ranging from 1 to 1000 s^{-1}. The viscosity of the solution (c = 1 mg/mL, η_{rel} = 3.0) showed a distinct drop in viscosity at shear rates above 200 s^{-1} before reaching a secondary Newtonian plateau, that is, the chitin solutions are shear thinning. In the capillary viscosimeter used in our experiments, the shear rate is ~110 s^{-1}, which confirms Newtonian flow behavior for all the chitin samples in the capillary during the viscometric measurements.

3.4. Dynamic Light Scattering of Alkali Chitin. The theory of dynamic light scattering can be found in many textbooks[11] and reviews.[12] We present here only the equations necessary for the present analysis. The intensity autocorrelation function of the scattered light $g^{(2)}(\tau)$ is given by

$$g^{(2)}(\tau) = \frac{\langle I(t)\, I(t+\tau)\rangle}{\langle I(t)\rangle^2} \tag{3}$$

where $I(t)$ and $I(t + \tau)$ are the intensity of the scattered light at time t and $t + \tau$, respectively. The braces indicate time average. This correlation function is connected to the electric field autocorrelation function $g^{(1)}(\tau)$ by the Siegert relation

$$g^{(2)}(\tau) = B(1 + \beta[g^{(1)}(\tau)]^2) \tag{4}$$

where B denotes the baseline and β denotes the coherence factor. The electric field correlation function provides information about the translational diffusion coefficient D_T, because

$$g^{(1)}(\tau) = \int_0^\infty G(\Gamma)\mathrm{e}^{-\Gamma\tau}\,\mathrm{d}\Gamma \tag{5}$$

where $G(\Gamma)$ denotes the Γ distribution function and Γ is the decay rate given by $\Gamma = 1/\tau = D_T q^2$. Parameter q is the length of the scattering wave vector defined by

$$q = \frac{4\pi n}{\lambda}\sin\frac{\theta}{2} \tag{6}$$

where n is the refractive index of the solvent, λ is the vacuum wavelength of the laser light, and θ is the scattering angle. The Stokes−Einstein relation

$$D_T = \frac{k_B T}{6\pi\eta_s R_h} \tag{7}$$

can be used to relate the translational diffusion coefficient and the hydrodynamic radius, R_h, of spherical particles. Boltzmann's constant is denoted k_B, T is the absolute temperature, and η_s is the solvent viscosity. For nonspherical particles, the equation above gives the equivalent hydrodynamic radius of the particles.

Inverse Laplace transformation of eq 5 using the CONTIN program[13] yields the distribution function $G(\Gamma)$. The distribution function for the six chitin samples versus the equivalent hydrodynamic radius is shown in Figure 4. The distribution functions move toward lower size versus degradation time, as expected. For chitin sample C-1, we observe some aggregates at $R_h \approx$ 300 nm, whereas samples C-2 to C-6 contain no aggregates. A possible explanation for this obser-

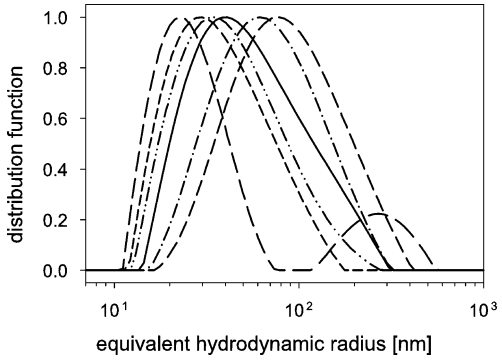

Figure 4. From dynamic light scattering data, the probability density of the equivalent hydrodynamic radius was obtained by the use of CONTIN. The chitin solutions are prepared from C-1 (long dashed line), C-2 (short dashed line), C-3 (dashed−dotted−dotted line), C-4 (solid line), C-5 (dashed−dotted line), and C-6 (medium-dashed line).

vation is that the aggregates in C1 are small enough to pass through the filter, whereas aggregates in C-2 to C-6 are too big.

Even though the C-1 aggregates are few in number, they will give a significant contribution to the total scattered light. A *z*-average parameter (R_g) is more affected by aggregates than a weight-average parameter (M_w). Therefore, on the basis of the size distributions obtained from dynamic light scattering data, we expect the estimated value for the *z*-average R_g to be too high in the sample with the lowest molecular weight, C-1.

From the size distribution shown in Figure 4, the average equivalent hydrodynamic radius and $\rho = R_g/R_h$ were calculated (Table 1). The parameter ρ describes to what extent a particle/polymer is drained by the solvent. Large drainage causes a reduction of the effective hydrodynamic radius, and ρ increases. If, on the other hand, only a minor drainage is possible, ρ decreases and approaches the value of 0.77 for compact spheres with no drainage. The results presented in Table 1 show a minor increase in ρ for C-5 and C-6.

3.5. Static Light Scattering of Alkali Chitin. From static light scattering measurements, Zimm plots were obtained by plotting Kc/R_θ versus $q^2 + kc$

$$\frac{Kc}{R_\theta} = \frac{1}{M_w}\left[1 + \frac{(qR_\theta)^2}{3}\right][1 + 2A_2M_wc] \qquad (8)$$

where R_θ is the Rayleigh ratio, A_2 is the second virial coefficient, and K is an instrument constant defined by

$$K = \frac{4\pi^2n^2(\partial n/\partial c)^2}{N_A\lambda^4} \qquad (9)$$

Here, N_A is Avogadro's number.

To investigate the effect of filtering during the preparation of the samples, chitin sample C-6 was filtered using different filter pore sizes. The molecular parameters obtained from the associated Zimm plots are given in Table 2. The molecular weight and the radius of gyration increase when the filter pore size is increased, as expected. Even though the aggregates are few in number, they contribute significantly to the total scattered light. Therefore, it is crucial to remove such aggregates from the sample before carrying out light scattering measurements. From these observations, we concluded that the filter pore size of 0.45 μm was the most appropriate for our samples. For the 0.1 μm filter, the pore size is of the same order of magnitude as the chitin molecule; thus, this is an improper choice of filter. The second virial coefficients of the chitin solutions have values as expected for molecular disperse solutions.[14]

Table 1. Average Equivalent Hydrodynamic Radius and $\rho = R_g/R_h$ for the Chitin Samples after Different Degradation Times

chitin sample	degradation time [h]	R_h [nm]	ρ
C-1	345	34	1.1
C-2	48	37	1.1
C-3	24	43	1.1
C-4	12	53	1.1
C-5	3	67	1.2
C-6	0	84	1.3

Table 2. Molecular Parameters for Chitin Sample C-6 for Different Filter Pore Sizes[a]

filter pore size [μm]	M_w [kg/mol]	R_g [nm]	A_2 [mL·mol·g^{-2}]
0.45	1200	110	1.2×10^{-3}
1.2	1400	120	1.1×10^{-3}
5.0	1600	130	1.3×10^{-3}

[a] The molecular weight, radius of gyration, and second virial coefficient are determined from Zimm plots. In these measurements, we used filters from an Acrodisc with Versapor membrane.

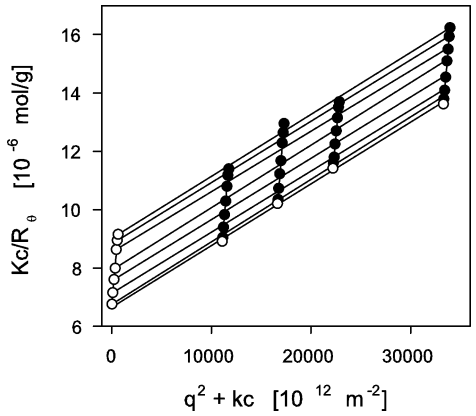

Figure 5. Zimm plot for chitin solutions made from sample C-2. The experimental data are denoted ●, and the extrapolated values are denoted ○.

For each Zimm plot, four to six different concentrations of chitin were used. The Zimm plots for chitin samples C-2, C-4, and C-6 are shown in Figures 5−7, respectively. Extrapolation to zero angle against *c* and to zero concentration against q^2 gave linear plots. From these straight lines, the weight-average molecular weight, the *z*-average radius of gyration, and the second virial coefficient were calculated in the customary manner (Table 3). The molecular weight and radius of gyration decrease as a function of degradation time as expected. The second virial coefficient is positive and between 1 and 2 $\times$ 10^{-3} mL·mol·g^{-2} for all chitin samples, that is, no significant aggregation takes place for the used range of concentrations and 2.77 M NaOH is a good solvent to chitin.

3.6. Relation between Intrinsic Viscosity and Molecular Weight. The results in Table 3 were used to determine the parameters of the MHS equation by plotting log([η]) versus

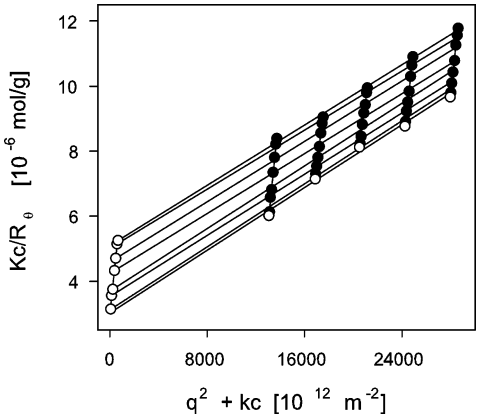

Figure 6. Zimm plot for chitin solutions made from sample C-4. The experimental data are denoted ●, and the extrapolated values are denoted ○.

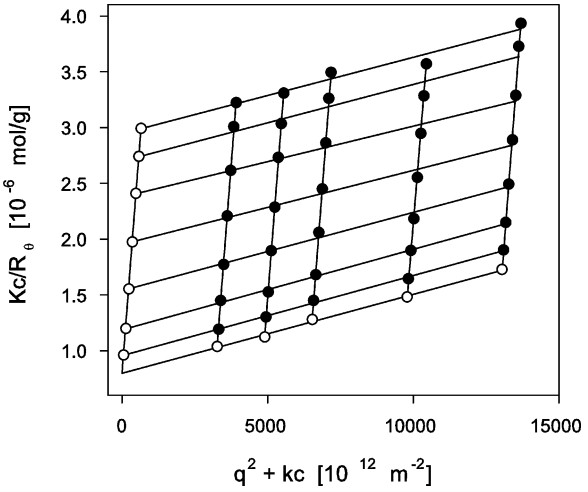

Figure 7. Zimm plot for chitin solutions made from sample C-6. The experimental data are denoted ●, and the extrapolated values are denoted ○.

Table 3. Molecular Parameters for Chitin after Different Degradation Times[a]

chitin sample	degradation time [h]	M_w [kg/mol]	R_g [nm]	A_2 [mL·mol·g^{-2}]	[η] [mL/g]
C-1	345	100	38	2.05×10^{-3}	237
C-2	48	150	42	1.95×10^{-3}	327
C-3	24	200	48	2.02×10^{-3}	408
C-4	12	330	60	2.23×10^{-3}	528
C-5	3	640	82	2.13×10^{-3}	831
C-6	0	1200	110	1.23×10^{-3}	1354

[a] The molecular weight, radius of gyration, and second virial coefficient are determined from static light scattering. The intrinsic viscosity is calculated from viscometric measurements.

log(M_w) for the six chitin samples (Figure 8). Parameter *a* was obtained from the slope of this double logarithmic plot. The value of *K* was obtained from extrapolation. The correlation coefficient of 0.9971 for the curve in Figure 8 signifies an excellent linearity of the MHS equation obtained

$$[\eta] = 0.10M_w^{0.68}\ (\text{mL/g}) \tag{10}$$

The value of exponent *a* indicates that chitin has a random-coil structure and that the solvent properties are fairly good.

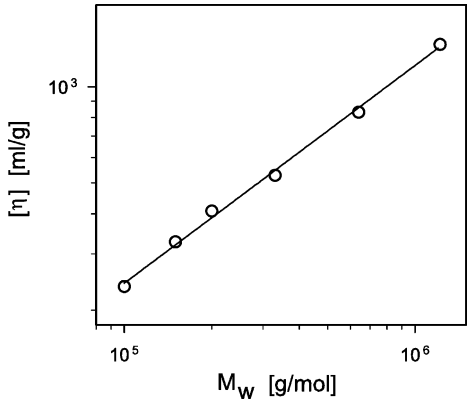

Figure 8. Plot of [η] versus M_w for chitin solutions prepared from samples C-1 to C-6. These data were used to determine the parameters *a* and *K* of the MHS equation. The experimental data are denoted ○, and the solid line is the regression line. The correlation coefficient for the fit is 0.9971.

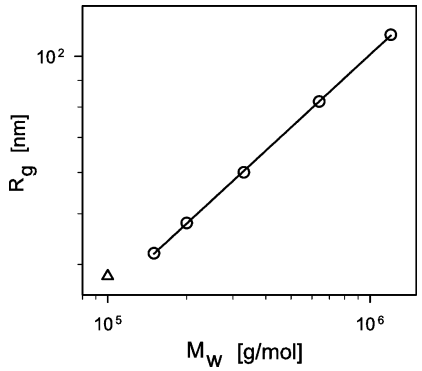

Figure 9. Plot of R_g versus M_w for chitin solutions prepared from samples C-1 to C-6. The experimental value for sample C-1, denoted by △, is not included in the regression analysis. The experimental values for samples C-2 to C-6 are denoted ○, and the solid line is the regression line for C-2 to C-6. The correlation coefficient for the fit is 0.9999.

3.7. Relation between Radius of Gyration and Molecular Weight. The radius of gyration R_g of a polymer is related to the molecular weight M_w by the equation

$$R_g = CM_w^b \tag{11}$$

where *C* and *b* for a given sample are empirical constants. The exponent *b* is a polymer conformation parameter that decreases with increasing molecular compactness. For spherical molecules, $b = 1/3$, and for long thin rodlike molecules, $b = 1$. For random-coil molecules, the value of *b* depends on the solvent. For a perfectly uncorrelated segmented chain, $b = 0.50$. A plot of log(R_g) versus log(M_w) is given in Figure 9. From the dynamic light scattering measurements, we concluded that aggregates were present in C-1. Figure 9 confirms the expectation that the estimated R_g value of C-1 is too high. Therefore, the experimental values for C-1, denoted by (Δ) in Figure 9, is not included in the regression analysis. Exponent *b* was obtained from the slope of a double logarithmic plot in Figure 9. The correlation coefficient of 0.9999 for the curve in Figure 9 signifies an excellent linearity of the equation obtained

$$R_g = 0.17M_w^{0.46}\ (\text{nm}) \tag{12}$$

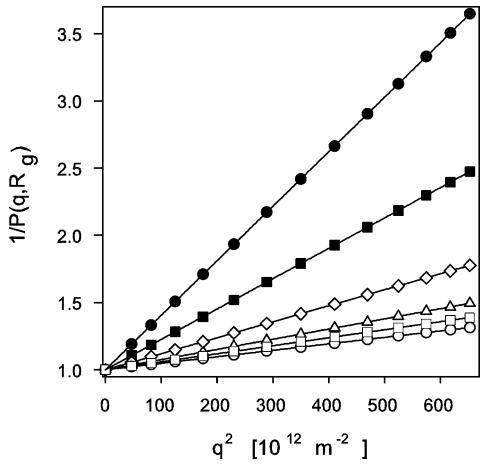

Figure 10. Plot of the theoretical values of $1/P(q, R_g)$ versus q^2 for random-coil structures that show polydispersity in molecular weight (solid lines). The experimental values for $1/P(q, R_g)$ for samples C-1 (○), C-2 (□), C-3 (△), C-4 (◇), C-5 (■), and C-6 (●) agree well with the theoretical predictions.

The value of the exponent in eq 12 is in agreement with the exponent a of 0.68 in the MHS equation, which gives further support to the random-coil structure of the chitin molecules in alkaline solutions. The chitin molecules are expected to be charged in 2.77 M NaOH, because their pK_a values are in the range from 12 to 14.[15] However, at such a high ionic strength, the presence of negative charges on neighboring units will have a minor affect on the conformation of the chains.

3.8. Particle Form Factor. The particle form factor $P(q, R_g)$ contains information about molecular shape. The function $P(q, R_g)$ has been calculated for molecules of several different shapes, in particular, thin rods, random coils, spheres, ellipsoids, and cylinders.[16]

The lines drawn in Figure 10 are the theoretical form factor curves for random-coil structure, polydisperse in molecular weight, calculated according to the formula

$$1/P(q, R_g) = 1 + \frac{(qR_g)^2}{3} \tag{13}$$

For all the chitin samples, the experimental values for $1/P(q, R_g)$ coincide with the theoretical curves (Figure 10). Chitin has a polydisperse random-coil structure regardless of the molecular weight in the studied range. None of the theoretical curves for other shapes fit the experimental data. The form factor for monodisperse random-coil structure was the second best choice

$$1/P(q, R_g) = \frac{(qR_g)^4}{2[(qR_g)^2 - 1 + \exp\{-(qR_g)^2\}]} \tag{14}$$

The absolute sum of squared errors (ASSE) between theoretical and experimental values for $1/P(q, R_g)$ for polydisperse and monodisperse random-coil structure is defined as

$$\mathrm{ASSE} = \sum_i \{[1/P(q, R_g)]_i^{\mathrm{theo}} - [1/P(q, R_g)]_i^{\mathrm{exp}}\}^2 \tag{15}$$

and the relative sum of squared errors (RSSE) is defined as

Table 4. Absolute and Relative Sum of Squared Errors (ASSE and RSSE) for Polydisperse and Monodisperse Random-Coil Structure, Given for the Six Chitin Samples

chitin sample	ASSE × 10^{-4} polydisperse	ASSE × 10^{-4} monodisperse	RSSE × 10^{-4} polydisperse	RSSE × 10^{-4} monodisperse
C-1	8	25	6	16
C-2	9	54	6	29
C-3	21	130	14	63
C-4	74	640	39	220
C-5	51	5300	17	840
C-6	40	33 000	10	2300

$$\mathrm{RSSE} = \sum_i \left\{ \frac{[1/P(q, R_g)]_i^{\mathrm{theo}} - [1/P(q, R_g)]_i^{\mathrm{exp}}}{[1/P(q, R_g)]_i^{\mathrm{theo}}} \right\}^2 \tag{16}$$

The ASSEs and RSSEs for polydisperse and monodisperse random-coil structure are given in Table 4. The RSSE values calculated for the six chitin samples, assuming a polydisperse random-coil structure, show no systematic significant change with increasing M_w; that is, a polydisperse random-coil structure yields a good fit for all the samples. On the other hand, the RSSE values calculated for a monodisperse random-coil structure show a systematic significant increase with increasing M_w.

3.9. Chain Dimensions. The number of Kuhn statistical segments N_k and the length of the Kuhn statistical segment Q_k are determined by the equations

$$N_k Q_k^2 = \langle r_{e-e}^2 \rangle \tag{17}$$

$$N_k Q_k = L_c \tag{18}$$

where $\langle r_{e-e}^2 \rangle$ is the mean square end-to-end distance and L_c is the contour length. The radius of gyration and the mean square end-to-end distance for an uncorrelated segmented chain is related through

$$R_g^2 = \frac{N_k + 2}{6(N_k + 1)} \langle r_{e-e}^2 \rangle \tag{19}$$

The contour length of the chitin molecules is given by

$$L_c = \frac{M_w}{M_{mon}} L_{mon} \tag{20}$$

where L_{mon} is the length of a projection of the repeating unit on the chitin chain axis and M_{mon} is the molecular weight of the repeating unit in chitin. We assume that $L_{mon} = 0.514$ nm and $M_{mon} = 203$ g/mol.[5,17,18] The radius of gyration and the molecular weight obtained from light scattering experiments and eqs 17−20 yield N_k, Q_k, and L_c (Table 5).

The length of the Kuhn statistical segment describes the local chain stiffness. Provided that the physical properties are the same along the chain, this length should be identical for all samples of the same polymer. From Table 5, we observe that Q_k slightly decreases versus M_w. This is in perfect agreement with the experimental data shown in Figure 9. The exponent b equals 0.46 for our chitin samples; that is, chitin is not a perfect uncorrelated segmented polymer chain. Ignoring sample C-1, for the same reason as discussed in section 3.7, we obtain Q_k in the range from 23 to 26 nm.

Table 5. Number of Kuhn Statistical Segments N_k, the Length of the Kuhn Statistical Segment Q_k, the Contour Length L_c, the Linear Expansion Factor α_s, the Unperturbed Chain Dimension A and the Characteristic Ratio C_∞[a]

sample	degradation time [h]	N_k	Q_k [nm]	L_c [nm]	α_s	A [nm]	C_∞
C-1	345	8.2	30.9	253	1.02	0.29	64
C-2	48	14.5	26.2	380	1.03	0.26	51
C-3	24	19.5	26.0	506	1.04	0.25	49
C-4	12	33.3	25.1	836	1.06	0.24	44
C-5	3	65.9	24.6	1620	1.10	0.23	40
C-6	0	132.4	23.3	3089	1.08	0.23	39
chitin[5]					1.01	0.38	113
cellulose[4]					1.03	0.41	92

[a] The values of alkali chitin are compared to the values of chitin and cellulose in DMAc−LiCl.

The unperturbed chain dimension A and the characteristic ratio C_∞ are determined by

$$A = \left(\frac{\langle r_{e-e}^2 \rangle_0}{M_w} \right)^{1/2} \tag{21}$$

and

$$C_\infty = \frac{\langle r_{e-e}^2 \rangle_0}{n L_{mon}^2} \tag{22}$$

where $\langle r_{e-e}^2 \rangle_0$ is the unperturbed mean square end-to-end distance and $n = M_w/M_{mon}$ is the number of main-chain bonds. The linear expansion factor α_s, given by

$$\langle r_{e-e}^2 \rangle_0 = \frac{\langle r_{e-e}^2 \rangle}{\alpha_s} \tag{23}$$

is calculated by using the method in ref 4. The results for our chitin samples are given in Table 5. The A and C_∞ values obtained for chitin in alkali are lower than those of chitin and cellulose in DMAc−LiCl solvent[4,5] (Table 5), as expected because DMAc−LiCl enhances the stiffness of the chitin/cellulose backbone.

4. Conclusion

Dilute solution properties of chitin in alkali have been determined, showing that alkali is a good solvent to chitin and that the chitin molecules behave as random coils. This solvent system is an attractive alternative to previously described solvents to chitin, where aggregates and a more extended chain conformation have been observed.

Acknowledgment. We acknowledge funding from Norwegian Biopolymer Laboratory (NOBIPOL) and the Norwegian Research Council, Grants 138394/410, 143184/140, and 134674/I10.

References and Notes

(1) Austin, P. R. *Chem. Abstr.* **1978**, *88*, 6349d.
(2) Sannan, T.; Kurita, K.; Iwakura, Y. *Die Makromolekulare Chemie* **1975**, *176*, 1191−1195.
(3) Flory, P. J. *Principles in polymer chemistry;* Cornell University Press: New York, 1953.
(4) McCormick, C. L.; Callais, P. A.; Hutchinson, B. H. *Macromolecules* **1985**, *18*, 2394−2401.
(5) Terbojevich, M.; Carraro, C.; Cosani, *A. Carbohydr. Res.* **1988**, *180*, 73−86.
(6) Einbu, A.; Vårum, K. M. Manuscript in preparation.
(7) Chu, B. *Laser light scattering. Basic principles and practice*, 2nd ed.; Academic Press: San Diego, 1993.
(8) Fredheim, G. E.; Christensen, B. E. *Biomacromolecules* **2003**, *4*, 232−239.
(9) Stokke, B. T.; Elgsaeter, A.; Bjørnestad, E. Ø.; Lund, T. *Carbohydr. Poly.* **1992**, *17*, 209−220.
(10) Roberts, G. A. F. *Chitin Chemistry*; The Macmillan Press, Ltd.: London, 1992.
(11) Berne, B. J.; Pecora, R. *Dynamic light scattering*; Wiley: New York, 1976.
(12) Santos, N. C.; Castaho, M. A. R. B. *Biophys. J.* **1996**, *71*, 1641−1650.
(13) Provencher, S. W. *CONTIN (Version 2) Users manual*; Technical Report EMBL-DA07; Max-Planck-Institut Biophysikalische Chemie: Göttingen, 1984.
(14) Tanford, C. *Physical Chemistry of Macromolecules*; John Wiley: New York, 1961.
(15) Rendleman, J. A. J. *Adv. Carbohydr. Chem.* **1973**, *117*, 51−69.
(16) Geiduschek, E. P.; Holtzer, A. *Adv. Biol. Med. Phys.* **1958**, *6*, 431−549.
(17) Yamakawa, H.; Fujii, M. *Macromolecules* **1974**, *7*, 128−135.
(18) Carlstrom, D. *J. Biophys. Biochem. Cytol.* **1957**, *3*, 669−683.

BM049710D